

Fermi National Accelerator Laboratory

FN-453
1900.000

**Design of the
Transverse Current Emittance Monitor (XIEM)
Detector**

G. Jackson

Fermi National Accelerator Laboratory
P.O. Box 500
Batavia, IL 60510 USA

April 16, 1987



**DESIGN OF THE
TRANSVERSE CURRENT EMITTANCE MONITOR (XIEM)
DETECTOR**

G. Jackson 4/16/87

TABLE OF CONTENTS

I. Introduction	1.3
A. Summary	1.3
B. Motivation	1.4
C. Conventions	1.4
II. Electrodynamical Calculation	2.1
A. Geometry	2.1
B. Transverse Currents	2.3
C. Longitudinal Magnetic Field	2.5
III. Calculation of B_s	3.1
A. Basic Calculation	3.1
B. Including Dispersion	3.4
C. Including Steering Errors	3.8
IV. Main Ring XIEM Proposal	4.1
A. Detector Geometry and Locations	4.1
B. Signal Characteristics	4.5
C. Steering Error Compensation	4.9
D. Signal Processing	4.13
V. Test Stand Proposal	5.1

I. INTRODUCTION

A. Summary

Taking advantage of the transverse component of the beam current at a position in an accelerator lattice of nonzero Twiss parameter $\alpha_{x,y}$, an induced voltage of approximately $10 \mu\text{V}$ (assuming 8 GeV Main Ring conditions) is induced on each of four conductor loops. The combination of these voltages produces a signal linear in energy width and horizontal and vertical emittance. In the same way as two flying wires are needed to discriminate between the betatron and energy widths of beams, three XIEM detectors can provide independent measures of all three phase space emittances. The sensitivity to beam steering errors is examined, and is found to be negligible when a compensation scheme is employed.

This paper is organized into five chapters. The second chapter introduces the concept of transverse current densities, and suggests the idea of using the longitudinal magnetic field generated by these currents as a means of measuring transverse emittance. The third chapter of this document describes the calculation of this longitudinal magnetic field (B_S). Chapter four describes the proposed Main Ring XIEM monitor. Chapter five is a test stand proposal for first testing the calculations presented in this paper.

B. Motivation

The two beam parameters which determine colliding beam luminosity are the beam current and emittances. Beam current detectors are plentiful, but to date the only transverse emittance monitors available are intrusive in nature. Secondary Emission Monitors (SEMs) are purely single pass (beamline) detectors, and flying wires provide only time averaged information (hence they assume an equilibrium, steady-state beam distribution). A bunch-by-bunch, turn-by-turn transverse emittance monitor would be an invaluable tool for both accelerator studies and real-time luminosity calculations.

C. Conventions

Due to an acute shortage of unique symbols in physics, this document will define quantities in terms of the arguments and subscripts. For example, $\beta_x(s)$ will refer to the general beta function around the ring, while β_x refers to the value of the β -function at the detector location ($s=0$). As another example, the relativistic quantities $\beta = v/c$ and $\gamma = E/mc^2$ are distinguished from the Twiss parameters $\beta_{x,y}$ and $\gamma_{x,y}$ by the use of subscripts.

II. ELECTRODYNAMICAL CALCULATION

A. Geometry

Imagine a relativistic particle bunch ($\gamma \gg 1$) circulating in an accelerator, passing a designated location ($s=0$) characterized by the Twiss parameters $\alpha_{x,y}$, $\beta_{x,y}$, and $\gamma_{x,y}$. For the time being, it will be assumed that the dispersion is zero at this location. In addition, assume that the bunch does not execute coherent betatron motion. The evolution of the bunch cross section in a drift section is calculated using the equations¹.

$$\sigma_{x,y}(s) = \sqrt{\epsilon_{x,y} \beta_{x,y}(s)} \quad , \quad (2.1)$$

$$\beta_{x,y}(s) = \beta_{x,y} - 2 s \alpha_{x,y} + s^2 \gamma_{x,y} \quad , \quad (2.2)$$

where $\epsilon_{x,y}$ are the horizontal and vertical bunch emittances. Figure 2.1 is a sketch of the the bunch cross section at, and one meter before and after, the F13 Main Ring BPM location. Since the bunch cross section is changing, particles must be flowing transversely. Therefore transverse currents exist at that location in the accelerator.

1. E.Courant and H.Snyder, "Theory of the Alternating-Gradient Synchrotron", Annals of Physics 3, 1 (1958).

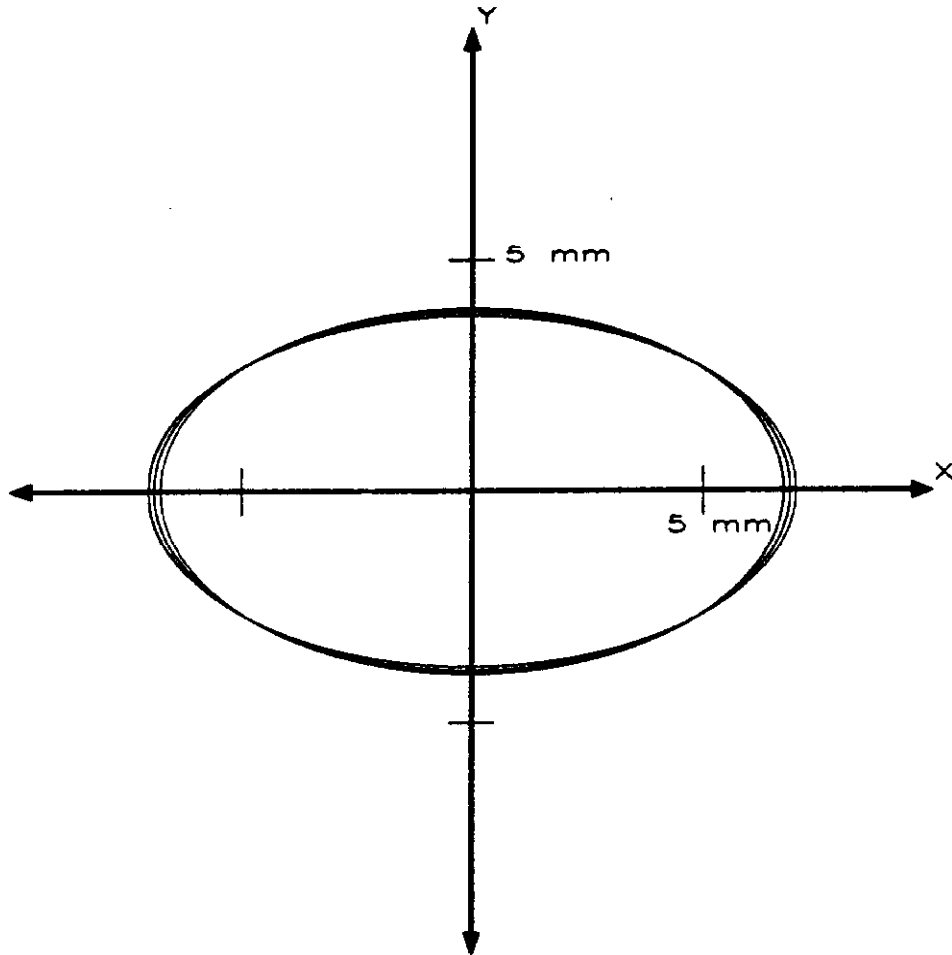


Figure 2.1: Sketch of the rms transverse cross section of a typical Main Ring proton bunch at, and one meter before and after, the F13 BPM location.

B. Transverse Currents

Assume a general phase space charge distribution $\rho(x,p,y,q,s,\delta;t)$. The spatial charge and current densities are

$$\rho(x,y,s;t) = \int_{-\infty}^{+\infty} \rho(x,p,y,q,s,\delta;t) dp dq d\delta \quad , \quad (2.3)$$

and
$$J_s(x,y,s;t) = c \rho(x,y,s;t) \quad , \quad (2.4)$$

$$J_x(x,y,s;t) = \frac{-c \alpha_x(s)}{\beta_x(s)} x \rho(x,y,s;t) \quad , \quad J_y(x,y,s;t) = \frac{-c \alpha_y(s)}{\beta_y(s)} y \rho(x,y,s;t) \quad (2.5)$$

The horizontal position and angle are x and p , y and q are the vertical position and angle, s is the longitudinal position, and δ is the fractional energy error.

As an example calculation, assume a Gaussian proton bunch. The phase space charge distribution at a longitudinal accelerator location $s'=0$, in the rest frame of the bunch (K'), is

$$\rho'(x,p,y,q,s',\delta;t') = \frac{N e}{(2\pi)^{5/2} \epsilon_x \epsilon_y \sigma_\delta \sigma_{s'}} \exp \left[- \frac{a^2}{2\epsilon_x} - \frac{b^2}{2\epsilon_y} - \frac{\delta^2}{2\sigma_\delta^2} - \frac{(s'-ct')^2}{2\sigma_{s'}^2} \right] \quad , \quad (2.6)$$

where $\sigma_{s'}$ is the bunch length measured in the rest frame and

$$\begin{aligned} a^2 &= \gamma_x(s') x^2 + \beta_x(s') p^2 + 2 \alpha_x(s') x p \quad , \\ b^2 &= \gamma_y(s') y^2 + \beta_y(s') q^2 + 2 \alpha_y(s') y q \quad . \end{aligned} \quad (2.7)$$

Applying the integration outlined in equation 2.3 to equations 2.6 and 2.7 yields a spatial charge density of

$$\rho'(x,y,s';t') = \frac{N e}{(2\pi)^{3/2} \sigma_x(s') \sigma_y(s') \sigma_s} \exp \left[-\frac{x^2}{2\sigma_x^2(s')} - \frac{y^2}{2\sigma_y^2(s')} - \frac{(s'-ct')^2}{2\sigma_s^2} \right]. \quad (2.8)$$

To calculate the charge and current densities in the lab frame (K), the charge and current densities in the bunch rest frame must be Lorentz transformed² via

$$\begin{pmatrix} c\rho \\ J_x \\ J_y \\ J_s \end{pmatrix} = \begin{pmatrix} \gamma & 0 & 0 & \gamma\beta \\ 0 & 1 & 0 & 0 \\ 0 & 0 & 1 & 0 \\ \gamma\beta & 0 & 0 & \gamma \end{pmatrix} \begin{pmatrix} c\rho' \\ J_x' \\ J_y' \\ J_s' \end{pmatrix}. \quad (2.9)$$

Since the K' frame is the rest frame, by definition $J_s' = 0$. Assume that the bunch velocity is $\beta = 1$. Then equation 2.9 requires that

$$\rho(x,y,s;t) = \frac{N e}{(2\pi)^{3/2} \sigma_x(s) \sigma_y(s) \sigma_s} \exp \left[-\frac{x^2}{2\sigma_x^2(s)} - \frac{y^2}{2\sigma_y^2(s)} - \frac{(s-ct)^2}{2\sigma_s^2} \right], \quad (2.10)$$

where σ_s is now the bunch length measured in the lab frame. In addition

$$J_s(x,y,s;t) = c \rho(x,y,s;t). \quad (2.11)$$

Since $\rho(x,y,s;t)$ and $J_s(x,y,s;t)$ are known, $J_x(x,y,s;t)$ and $J_y(x,y,s;t)$ can be calculated using the continuity equation

$$\vec{\nabla} \cdot \vec{J} + \frac{\partial \rho}{\partial t} = 0. \quad (2.12)$$

2. J.D.Jackson, Classical Electrodynamics, John Wiley & Sons (1975), pg. 544.

Plugging equations 2.10 and 2.11 into 2.12, and splitting up the result into two equations (each either explicitly dependent on σ_x or σ_y),

$$\begin{aligned} \frac{\partial}{\partial x} J_x(x,y,s;t) &= \frac{c \rho(x,y,s;t)}{\beta_x(s)} \left[1 - \frac{x^2}{\sigma_x^2(s)} \right] (\gamma_x s - a_x) \quad , \\ \frac{\partial}{\partial y} J_y(x,y,s;t) &= \frac{c \rho(x,y,s;t)}{\beta_y(s)} \left[1 - \frac{y^2}{\sigma_y^2(s)} \right] (\gamma_y s - a_y) \quad . \end{aligned} \tag{2.13}$$

Integration over x and y from zero out to the transverse position of interest finally yields the result in equation 2.5.

C. Longitudinal Magnetic Field

Now that the existence of transverse currents is established, the resultant magnetic fields they produce must be examined. Since the transverse currents exist because of transverse emittance, and since the purpose of this exercise is to find a signal proportional to transverse bunch emittance, a component of the magnetic field uniquely generated by these currents (as opposed to fields generated by the forward motion of the beam) are of interest. Since the azimuthal magnetic field circulating around the bunch charge distribution is quite large, the only component available is the longitudinal magnetic field (B_s).

Assume that $a_x < 0$ and that $a_y = 0$. The transverse currents are then purely horizontal. Imagine that the beam is infinitesimally short and high. The horizontal current density can then be modelled as current segments flowing outward. Figure 2.2 is a sketch of this model, with B_s indicated at

four locations. Note that B_s is odd in both x and y . By repeating the above argument in the vertical plane, the same pattern is found, but with opposite sign.

Clearly B_s exists, and is generated uniquely by phase space emittance. The next steps in this design report are to calculate this field analytically, and to design a detector which couples into it.

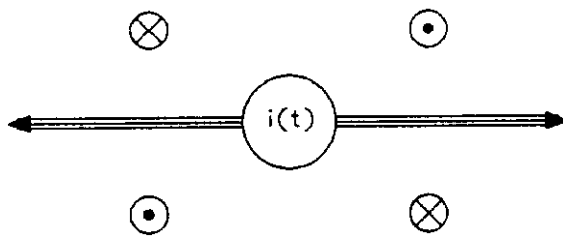


Figure 2.2: Model of a beam only spreading horizontally ($a_x < 0$ and $a_y = 0$), with the longitudinal magnetic field indicated near the current segments representing both halves of the beam.

III. CALCULATION OF B_S

A. Basic Calculation

In principle it should be possible to take the transverse current densities in equation 2.5 and calculate the longitudinal magnetic field B_S using the relationship

$$\vec{B}(\vec{x}) = \vec{\nabla} \times \vec{A}(\vec{x}) = \vec{\nabla} \times \frac{1}{c} \int_{-\infty}^{\infty} d^3x' \frac{\vec{J}(\vec{x}')}{|\vec{x} - \vec{x}'|} \quad (3.1)$$

In reality the integral can only be solved explicitly for very special cases, and certainly not for reasonable beam distributions (such as elliptical or Gaussian). Therefore another calculational method is used to find the equation describing the magnitude of B_S at some observation point (x_0, y_0, s_0) .

The magnitude of the longitudinal component of the magnetic field generated by a single proton with phase space coordinates (x, p, y, q, s) , in a region of zero dispersion, is

$$B_S(x, p, y, q, s | x_0, y_0, t) = \frac{\mu_0 e c}{2\pi} \delta(s-ct) \frac{q(x-x_0) - p(y-y_0)}{(x-x_0)^2 + (y-y_0)^2} \quad (3.2)$$

The δ -function in equation 3.2 reflects the assumption that the proton is relativistic ($\gamma \gg 1$), and that the bunch length is much longer than the typical transverse dimension of interest ($\sigma_S \gg x_0, y_0$). $\mu_0/4\pi$ is equal to 1×10^{-7} weber/Amp-m. By summing up the individual contributions of all the protons in the bunch, the total longitudinal magnetic field can be calculated. This summation over individual particles can be written as the integral of B_S in equation 3.2 times the proton phase space distribution

$$B_S(x_0, y_0, t) = \int_{-\infty}^{+\infty} \rho(x, p, y, q, s) B_S(x, p, y, q, s | x_0, y_0, t) dx dp dy dq ds \quad (3.3)$$

Since the protons are relativistic the longitudinal dependence of the Twiss parameters can be neglected, and integration over longitudinal phase space yields the result

$$B_S(x_0, y_0, t) = \frac{\mu_0 Ne e^{-t^2/2\sigma_\tau^2}}{(2\pi)^{7/2} \epsilon_x \epsilon_y \sigma_\tau} \int_{-\infty}^{\infty} dx dp dy dq \frac{q(x-x_0) - p(y-y_0)}{(x-x_0)^2 + (y-y_0)^2} \exp\left[\frac{-a^2}{2\epsilon_x} - \frac{b^2}{2\epsilon_y}\right], \quad (3.4)$$

where $\sigma_S = c\sigma_\tau$. The integration over p and q are carried out using the integral solutions

$$\int_{-\infty}^{\infty} \exp[-u^2 z^2 + 2vz] dz = \frac{\sqrt{\pi}}{u} \exp\left[\frac{v^2}{u^2}\right] \quad (u>0) \quad , \quad (3.5)$$

$$\int_{-\infty}^{\infty} z \exp[-u^2 z^2 + 2vz] dz = \frac{\sqrt{\pi}}{u} \exp\left[\frac{v^2}{u^2}\right] \frac{v}{u^2} \quad (u>0) \quad ,$$

producing the result

$$B_S(x_0, y_0, t) = \frac{\mu_0 Ne e^{-t^2/2\sigma_\tau^2}}{(2\pi)^{5/2} \sigma_x \sigma_y \sigma_\tau} \int_{-\infty}^{\infty} dx dy \frac{x(y-y_0)a_x/\beta_x - y(x-x_0)a_y/\beta_y}{(x-x_0)^2 + (y-y_0)^2} \exp\left[\frac{-x^2}{2\sigma_x^2} - \frac{y^2}{2\sigma_y^2}\right] \quad (3.6)$$

Rewrite the numerator of the integrand as

$$x_0(y-y_0) a_x/\beta_x - y_0(x-x_0) a_y/\beta_y + (x-x_0)(y-y_0)(a_x/\beta_x - a_y/\beta_y) \quad , \quad (3.7)$$

and assume that $\sigma_x > \sigma_y$. Then the integral solution

$$\frac{1}{2\pi \sigma_x \sigma_y} \int_{-\infty}^{\infty} dx dy \frac{e^{-x^2/2\sigma_x^2 - y^2/2\sigma_y^2}}{(x-x_0)^2 + (y-y_0)^2} \begin{Bmatrix} y-y_0 \\ x-x_0 \end{Bmatrix} = -\sqrt{\frac{\pi}{2(\sigma_x^2 - \sigma_y^2)}} \begin{Bmatrix} \text{Re} \\ \text{Im} \end{Bmatrix} f_{bb}(x_0, y_0, \sigma_x, \sigma_y) \quad (3.8)$$

where

$$f_{bb}(x_0, y_0, \sigma_x, \sigma_y) = W \left[\frac{x_0 + i y_0}{\sqrt{2(\sigma_x^2 - \sigma_y^2)}} \right] - \exp \left[\frac{-x_0^2}{2\sigma_x^2} - \frac{y_0^2}{2\sigma_y^2} \right] W \left[\frac{x_0 \sigma_y / \sigma_x + i y_0 \sigma_x / \sigma_y}{\sqrt{2(\sigma_x^2 - \sigma_y^2)}} \right] \quad (3.9)$$

allows the first two terms in equation 3.7 to be evaluated. The function f_{bb} is also used to describe the strength of the beam-beam force at a point in space generated by a Gaussian beam with $\sigma_x > \sigma_y$. The solution to the third term is

$$\frac{1}{2\pi \sigma_x \sigma_y} \int_{-\infty}^{\infty} dx dy \frac{(x-x_0)(y-y_0)}{(x-x_0)^2 + (y-y_0)^2} \exp \left[\frac{-x^2}{2\sigma_x^2} - \frac{y^2}{2\sigma_y^2} \right] = \quad (3.10)$$

$$-\sqrt{\frac{\pi}{2(\sigma_x^2 - \sigma_y^2)^3}} \left(x_0 \sigma_y^2 f_R(x_0, y_0, \sigma_x, \sigma_y) - y_0 \sigma_x^2 f_I(x_0, y_0, \sigma_x, \sigma_y) \right) \quad ,$$

where f_R and f_I are the real and imaginary parts of f_{bb} , and $\sigma_x > \sigma_y$.

Plugging in equations 3.8 and 3.10 into equation 3.6 yields the result

$$B_s(x_0, y_0, t) = \frac{-\mu_0}{4\pi} \frac{Ne}{\sqrt{2\pi} \sigma_\tau} e^{-t^2/2\sigma_\tau^2} \left\{ a_x \epsilon_x - a_y \epsilon_y \right\} \quad (3.11)$$

$$\cdot \sqrt{\frac{2\pi}{(\sigma_x^2 - \sigma_y^2)^3}} \left(x_0 f_R(x_0, y_0, \sigma_x, \sigma_y) - y_0 f_I(x_0, y_0, \sigma_x, \sigma_y) \right) \quad .$$

The factor on the second line is called g_s . When the beam aspect ratio σ_y/σ_x is close to one, it has the asymptotic limit

$$\lim_{x_o \gg \sigma_x} \left\{ \lim_{y_o \gg \sigma_y} \left\{ g_s \right\} \right\} = \frac{4 x_o y_o}{(x_o^2 + y_o^2)^2} \quad (3.12)$$

A detector far away from the beam center senses a longitudinal magnetic field whose magnitude is inversely proportional to the square of the detector radius, is linear in transverse emittance (since g_s is independent of either beam dimension), and is odd in both transverse planes (in agreement with the right-hand-rule derived B_s polarities shown in figure 2.2).

B. Including Dispersion

The magnitude of the longitudinal component of the magnetic field generated by a single proton with phase space coordinates (x,p,y,q,s) , in a region now with dispersion $(\eta_x, \eta'_x, \eta_y, \eta'_y)$, is

$$B_s(x,p,y,q,s|x_o,y_o,t) = \frac{\mu_o e c}{2\pi} \delta(s-ct) \frac{(q+\eta'_y \delta)(x-x_o+\eta_x \delta) - (p+\eta'_x \delta)(y-y_o+\eta_y \delta)}{(x-x_o+\eta_x \delta)^2 + (y-y_o+\eta_y \delta)^2} \quad (3.13)$$

Basically, equation 3.13 is identical to its zero dispersion counterpart equation 3.2, except that the energy contribution to the particle position and angle is included.

Plugging equation 3.13 into

$$B_s(x_o,y_o,t) = \int_{-\infty}^{+\infty} \rho(x,p,y,q,s,\delta) B_s(x,p,y,q,s,\delta|x_o,y_o,t) dx dp dy dq ds d\delta \quad (3.14)$$

produces the total beam induced longitudinal magnetic field. Following the same prescription as in section 3.A for the basic B_s calculation, equation 3.14 is reduced to

$$B_s(x_o, y_o, t) = \frac{-\mu_o}{4\pi} \frac{N e}{2\pi \sigma_\delta \sigma_\tau} \sqrt{\frac{2\pi}{\sigma_x^2 - \sigma_y^2}} e^{-t^2/2\sigma_\tau^2} \cdot \quad (3.15)$$

$$\cdot \int_{-\infty}^{\infty} d\delta e^{-\delta^2/2\sigma_\delta^2} \left\{ \left[\eta_y \delta - (y_o - \eta_y \delta) \frac{a_x \epsilon_x - a_y \epsilon_y}{\sigma_x^2 - \sigma_y^2} \right] f_I(x_o - \eta_x \delta, y_o - \eta_y \delta, \sigma_x, \sigma_y) + \right.$$

$$\left. - \left[\eta_x \delta - (x_o - \eta_x \delta) \frac{a_x \epsilon_x - a_y \epsilon_y}{\sigma_x^2 - \sigma_y^2} \right] f_R(x_o - \eta_x \delta, y_o - \eta_y \delta, \sigma_x, \sigma_y) \right\} ,$$

where $\sigma_x > \sigma_y$.

The integrals necessary to do the δ integration are¹

$$\int_{-\infty}^{\infty} \exp\left(\frac{-x^2}{2\sigma^2}\right) W(z + a x) dx = \frac{\sqrt{2\pi} \sigma}{\sqrt{1 + 2\sigma^2 a^2}} W\left(\frac{z}{\sqrt{1 + 2\sigma^2 a^2}}\right) \quad (3.16)$$

and

$$\int_{-\infty}^{\infty} x \exp\left(\frac{-x^2}{2\sigma^2}\right) W(z + a x) dx = \frac{2^{3/2} a \sigma^3}{1 + 2\sigma^2 a^2} \left[i - \frac{\sqrt{\pi} z}{\sqrt{1 + 2\sigma^2 a^2}} W\left(\frac{z}{\sqrt{1 + 2\sigma^2 a^2}}\right) \right] \quad (3.17)$$

Applying these integrals to equation 3.15 produces a very, very messy result.

In order to simplify the answer, the following definitions are necessary.

First, let

$$\sigma_{xy}^2 = \left(\sigma_x^2 + \eta_x^2 \sigma_\delta^2 \right) - \left(\sigma_y^2 + \eta_y^2 \sigma_\delta^2 \right) , \quad \xi^2 = 2 \eta_x \eta_y \sigma_\delta^2 \quad (3.18)$$

1. R.Meller, Private Communication (1984).

A measure of the effect of dispersion to the response of an XIEM detector is the parameter

$$\Delta = 1 + \frac{\eta_x^2 \sigma_\delta^2}{\sigma_x^2} + \frac{\eta_y^2 \sigma_\delta^2}{\sigma_y^2} \quad (3.19)$$

The primary form factor, similar to f_{bb} in equation 3.9, is

$$f_{bb}(x_o, y_o, \sigma_x, \sigma_y, \sigma_\delta, \eta_x, \eta_y) = W \left[\frac{x_o + iy_o}{\sqrt{2(\sigma_{xy}^2 + i\xi^2)}} \right] + \exp \left[-\frac{x^2}{2\sigma_x^2} - \frac{y^2}{2\sigma_y^2} + \frac{1}{2\Delta} \left[\frac{\eta_x \sigma_\delta x_o}{\sigma_x^2} + \frac{\eta_y \sigma_\delta y_o}{\sigma_y^2} \right]^2 \right] \quad (3.20)$$

$$\cdot W \left[\frac{\frac{\sigma_y}{\sigma_x} x_o + i \frac{\sigma_x}{\sigma_y} y_o + \frac{\eta_y^2 \sigma_\delta^2 x_o - \eta_x \eta_y \sigma_\delta^2 y_o}{\sigma_x \sigma_y} + i \frac{\eta_x^2 \sigma_\delta^2 y_o - \eta_x \eta_y \sigma_\delta^2 x_o}{\sigma_x \sigma_y}}{\sqrt{2\Delta(\sigma_{xy}^2 + i\xi^2)}} \right]$$

Finally, an ugly form factor which comes from the introduction of dispersion is

$$g_{bb}(x_o, y_o, \sigma_x, \sigma_y, \sigma_\delta, \eta_x, \eta_y) = \frac{-2i}{\sigma_{xy}^2 + i\xi^2} \left[\eta_x \sigma_\delta + i \eta_y \sigma_\delta \right] + \frac{-2i}{\sqrt{\Delta(\sigma_{xy}^2 + i\xi^2)}} \left[\frac{\sigma_x}{\sigma_y} \eta_x \sigma_\delta + i \frac{\sigma_y}{\sigma_x} \eta_y \sigma_\delta \right] \exp \left[-\frac{x^2}{2\sigma_x^2} - \frac{y^2}{2\sigma_y^2} + \frac{1}{2\Delta} \left[\frac{\eta_x \sigma_\delta x_o}{\sigma_x^2} + \frac{\eta_y \sigma_\delta y_o}{\sigma_y^2} \right]^2 \right] + \frac{\sqrt{\pi} f_{bb}(x_o, y_o, \sigma_x, \sigma_y, \sigma_\delta, \eta_x, \eta_y)}{(\sigma_{xy}^2 + i\xi^2)^{3/2}} \left[(x_o \eta_x \sigma_\delta - y_o \eta_y \sigma_\delta) + i (x_o \eta_y \sigma_\delta - y_o \eta_x \sigma_\delta) \right] \quad (3.21)$$

In terms of these parameters, the solution to equation 3.14 is

$$B_S(x_o, y_o, t) = \frac{-\mu_o}{4\pi} \frac{Ne}{\sqrt{2\pi} \sigma_\tau} e^{-t^2/2\sigma_\tau^2} \quad (3.22)$$

$$\left\{ \frac{\frac{\alpha_x \epsilon_x - \alpha_y \epsilon_y}{\sigma_x^2 - \sigma_y^2} \frac{\sqrt{\pi}}{\sqrt{\sigma_{xy}^2 + i\xi^2}} \left[x_o f_R(x_o, y_o, \sigma_x, \sigma_y, \sigma_\delta, \eta_x, \eta_y) - y_o f_I(x_o, y_o, \sigma_x, \sigma_y, \sigma_\delta, \eta_x, \eta_y) \right] + \right. \\ \left. - \frac{\frac{\alpha_x \epsilon_x - \alpha_y \epsilon_y}{\sigma_x^2 - \sigma_y^2} \left[\eta_x \sigma_\delta \mathcal{E}_R(x_o, y_o, \sigma_x, \sigma_y, \sigma_\delta, \eta_x, \eta_y) - \eta_y \sigma_\delta \mathcal{E}_I(x_o, y_o, \sigma_x, \sigma_y, \sigma_\delta, \eta_x, \eta_y) \right] + \right. \\ \left. - \left[\eta'_x \sigma_\delta \mathcal{E}_R(x_o, y_o, \sigma_x, \sigma_y, \sigma_\delta, \eta_x, \eta_y) - \eta'_y \sigma_\delta \mathcal{E}_I(x_o, y_o, \sigma_x, \sigma_y, \sigma_\delta, \eta_x, \eta_y) \right] \right\} .$$

Since B_S in equation 3.22 depends on both σ_δ and σ_τ , the XIEM detectors are theoretically capable of extracting all three phase space emittances from each bunch, each turn in the accelerator. As detailed in the next chapter, for locations in an accelerator where Δ is less than approximately 1.5, the response of an XIEM detector will be linear in σ_δ .

C. Including Steering Errors

Because real life is not perfect, the beams traversing the XIEM detectors will have average or coherent offsets (x_c, y_c) and angles (x_c', y_c') in both the horizontal and vertical planes. The inclusion of these errors in the equation for B_S is a trivial extension of the calculation in the previous section. Let

$$x_a = x_o - x_c \quad , \quad y_a = y_o - y_c \quad . \quad (3.23)$$

Then

$$B_S(x_a, y_a, t) = \frac{-\mu_o}{4\pi} \frac{Ne}{\sqrt{2\pi} \sigma_\tau} e^{-t^2/2\sigma_\tau^2} \quad . \quad (3.24)$$

$$\left\{ \frac{\frac{a_x \epsilon_x - a_y \epsilon_y}{\sigma_x^2 - \sigma_y^2} \frac{\sqrt{\pi}}{\sqrt{\sigma_{xy}^2 + i\xi^2}} \left[x_a f_R(x_a, y_a, \sigma_x, \sigma_y, \sigma_\delta, \eta_x, \eta_y) - y_a f_I(x_a, y_a, \sigma_x, \sigma_y, \sigma_\delta, \eta_x, \eta_y) \right] + \right. \\ - \frac{\frac{a_x \epsilon_x - a_y \epsilon_y}{\sigma_x^2 - \sigma_y^2}}{\sigma_x^2 - \sigma_y^2} \left[\eta_x \sigma_\delta g_R(x_a, y_a, \sigma_x, \sigma_y, \sigma_\delta, \eta_x, \eta_y) - \eta_y \sigma_\delta g_I(x_a, y_a, \sigma_x, \sigma_y, \sigma_\delta, \eta_x, \eta_y) \right] + \\ - \left[\eta_x' \sigma_\delta g_R(x_a, y_a, \sigma_x, \sigma_y, \sigma_\delta, \eta_x, \eta_y) - \eta_y' \sigma_\delta g_I(x_a, y_a, \sigma_x, \sigma_y, \sigma_\delta, \eta_x, \eta_y) \right] + \\ \left. - \frac{\sqrt{\pi}}{\sqrt{\sigma_{xy}^2 + i\xi^2}} \left[x_c' f_R(x_a, y_a, \sigma_x, \sigma_y, \sigma_\delta, \eta_x, \eta_y) - y_c' f_I(x_a, y_a, \sigma_x, \sigma_y, \sigma_\delta, \eta_x, \eta_y) \right] \right\} .$$

For locations (x_a, y_a) far away from the bunch center, the contribution to B_S from coherent angles is approximated quite well by assuming that the bunch is infinitesimally thin transversely (zero transverse emittance). This contribution can therefore be estimated using the equation

$$B_s(x_a, y_a, t) = \frac{\mu_0}{4\pi} \frac{Ne}{\sqrt{2\pi} \sigma_\tau} e^{-t^2/2\sigma_\tau^2} \frac{x'_c x_a - y'_c y_a}{x_a^2 + y_a^2} . \quad (3.25)$$

For typical Main Ring 8 GeV conditions, this contribution to the total longitudinal magnetic field can dominate the transverse emittance signal. In chapter 4 a scheme for cancelling away this effect is proposed.

IV. MAIN RING XIEM PROPOSAL

A. Detector Geometry and Locations

Figures 4.1 and 4.2 are the beam's eye and side views of the proposed Main Ring XIEM detector. Ignoring the detector wall and the transition section of the detector can, which transforms the beam pipe aspect ratio from a rectangle to a circle, the detector is simply a set of four conductor loops. The time derivative of the fraction of the longitudinal magnetic field B_s inside each loop induces an electromotive potential (EMF) according to

$$V(t) = - \frac{d}{dt} \int_{\text{enclosed}} B_s(x,y,t) \, dx dy \quad . \quad (4.1)$$

The dimensions of the loops and the wall are somewhat arbitrary, except that the Main Ring "minitube" horizontal aperture of 4" is maintained at the proposed detector location near the F13 beam position monitor (BPM) position.

The F13 BPM location was chosen as an acceptable detector location by examining the value of Δ (equation 3.19) around the ring (see figure 4.3). The values for the transverse emittances and energy spread represent typical 8 GeV conditions. Under optimum conditions, one would want to go to a Main Ring position where Δ was equal to unity (i.e. go to a location where the horizontal and vertical dispersion are equal to zero). Since that condition is never satisfied, a low value for Δ must be sufficient. In order to adequately test these detectors, the value of Δ at F13 (1.192) is somewhat larger than can be achieved at other Main Ring positions. The lattice

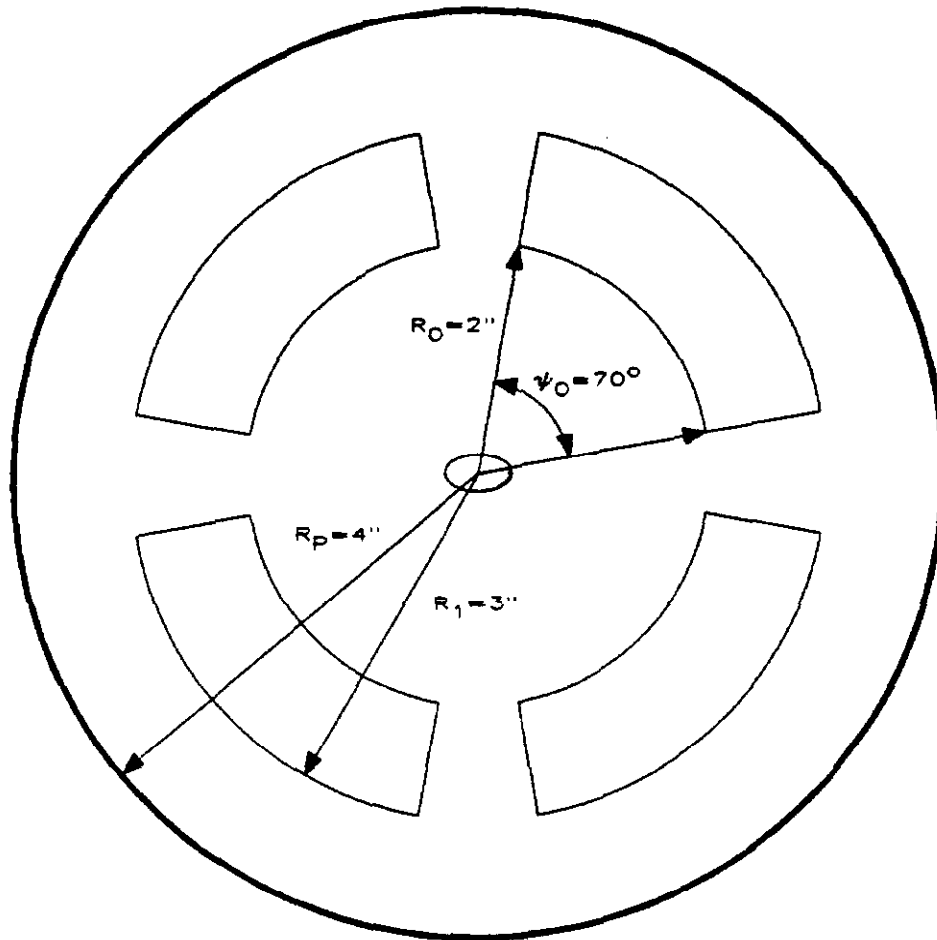


Figure 4.1: Beam's eye view of the proposed F13 XIEM detector. The four loops inside the circular beam pipe wall couple to the longitudinal component of the beam created magnetic field, inducing an EMF. The inner loop radius R_0 was chosen to preserve the 4" aperture of the F13 minitube.

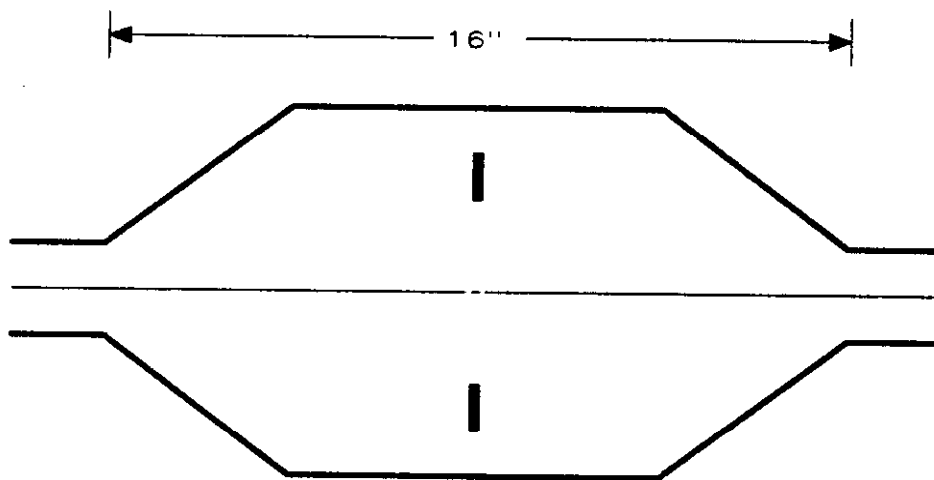


Figure 4.2: Side view of the proposed F13 XIEM detector. The sensing loops are characterized as short (or single turn) solenoids (an assumption justified later). The transition section on either side smoothly transforms the beam pipe cross section from a 2"x4" rectangle to a 6" radius circle.

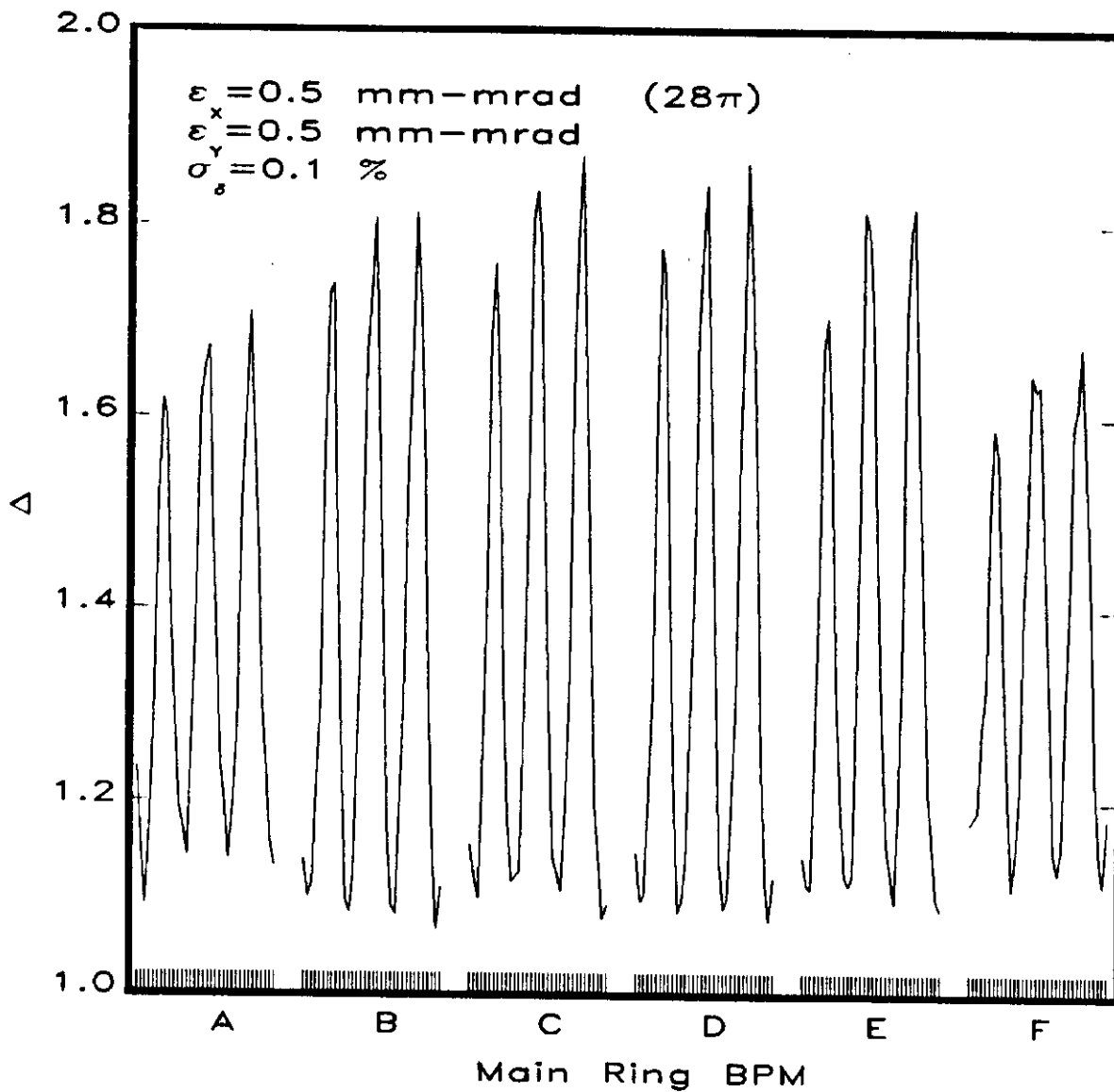


Figure 4.3: The value of the parameter Δ around the Main Ring at 8 GeV. Each point represents a BPM location.

parameters at the F13 BPM are:

$$\begin{array}{ll}
 \beta_x = 94.63 \text{ m} & \beta_y = 29.88 \text{ m} \\
 \alpha_x = 1.85 & \alpha_y = -0.58 \\
 \eta_x = 2.53 \text{ m} & \eta_y = -0.92 \text{ m} \\
 \eta'_x = -0.043 & \eta'_y = -0.019
 \end{array}$$

In order to independently measure the three bunch phase space emittances, three detectors are needed, where Δ , η_x , and η_y are different at each location. The dependence of B_s on all three emittances is quite linear over a large dynamic range of values when Δ is very close to one. Therefore, by evaluating $dV/d\epsilon_{x,y,s}$ at each detector, the three measured induced voltages (V_j) yield the three emittances (ϵ_i) via the matrix operation

$$\begin{pmatrix} \epsilon_x \\ \epsilon_y \\ \epsilon_z \end{pmatrix} = \begin{pmatrix} dV_1/d\epsilon_x & dV_1/d\epsilon_y & dV_1/d\epsilon_s \\ dV_2/d\epsilon_x & dV_2/d\epsilon_y & dV_2/d\epsilon_s \\ dV_3/d\epsilon_x & dV_3/d\epsilon_y & dV_3/d\epsilon_s \end{pmatrix}^{-1} \begin{pmatrix} V_1 \\ V_2 \\ V_3 \end{pmatrix} \quad (4.2)$$

B. Signal Characteristics

According to equation 4.1, the voltage waveform induced on each loop of the XIEM detector is the time derivative of the bunch charge distribution. Figure 4.4 is a sketch of the expected response under typical 8 GeV conditions, assuming only one conductor turn per loop. The minimum and maximum occur at the Gaussian inflection points ($\pm\sigma_T$). The transverse emittance and fractional bunch length dependence of the maximum voltage is shown in figures 4.5 and 4.6. Note that though not perfectly linear, a 5-10% number for each of the three bunch emittances using the scheme in equation 4.2 looks feasible.

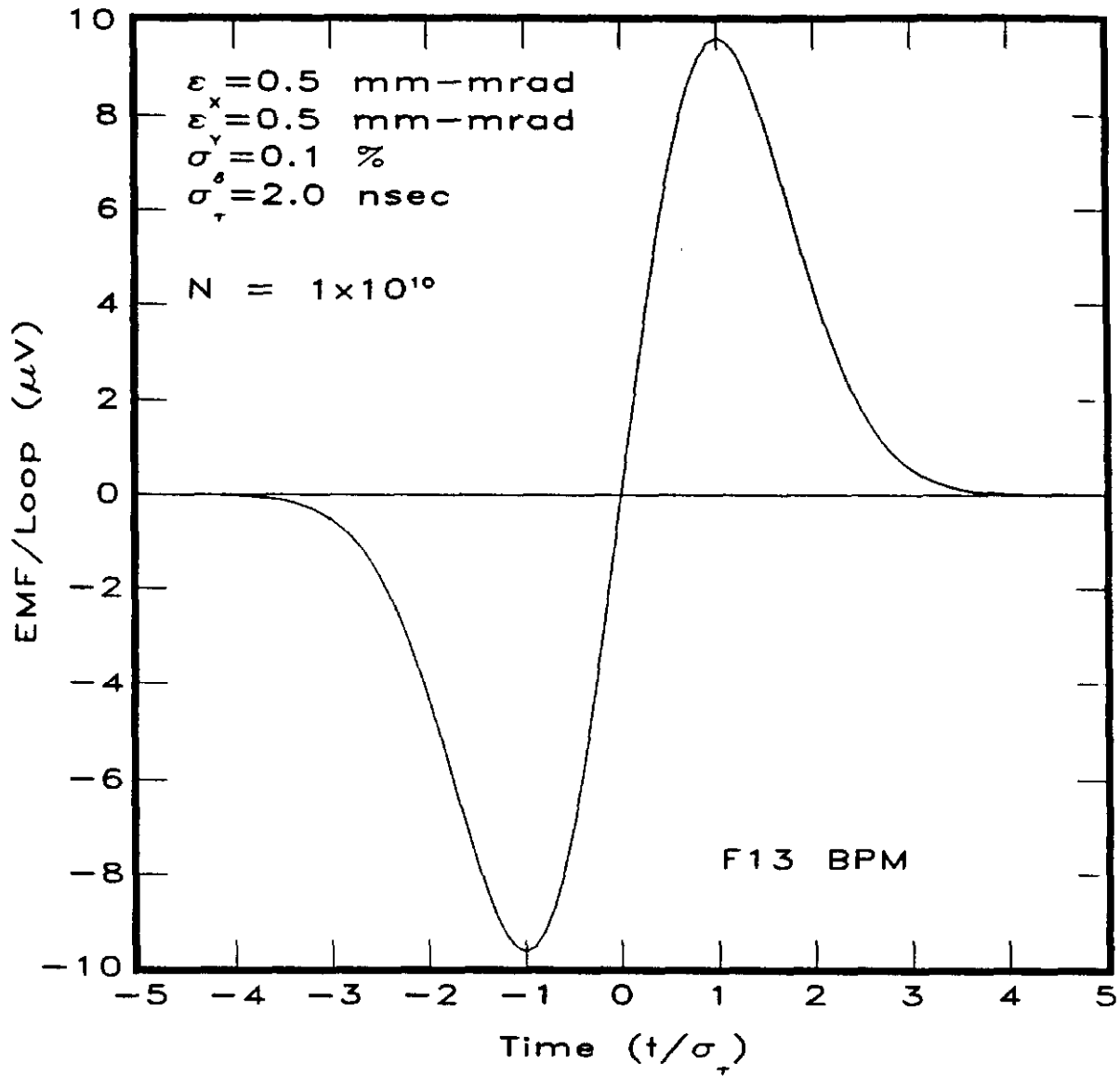


Figure 4.4: Calculated voltage waveform expected from a single loop in the proposed F13 XIEM detector. When the four loops are combined, the signal amplitude will be multiplied by 4.

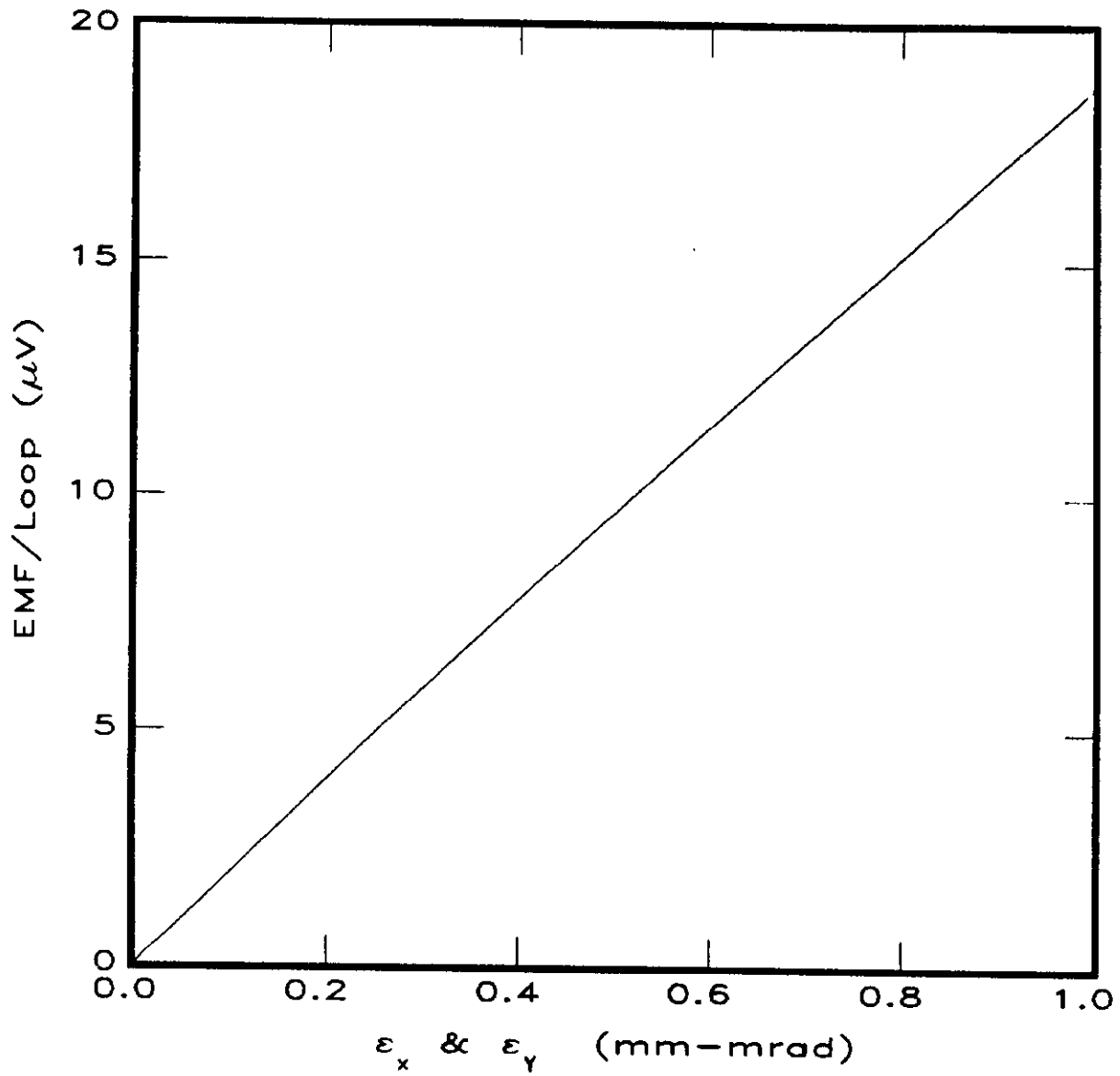


Figure 4.5: Dependence of the maximum voltage induced in a single F13 XIEM detector loop on transverse emittance.

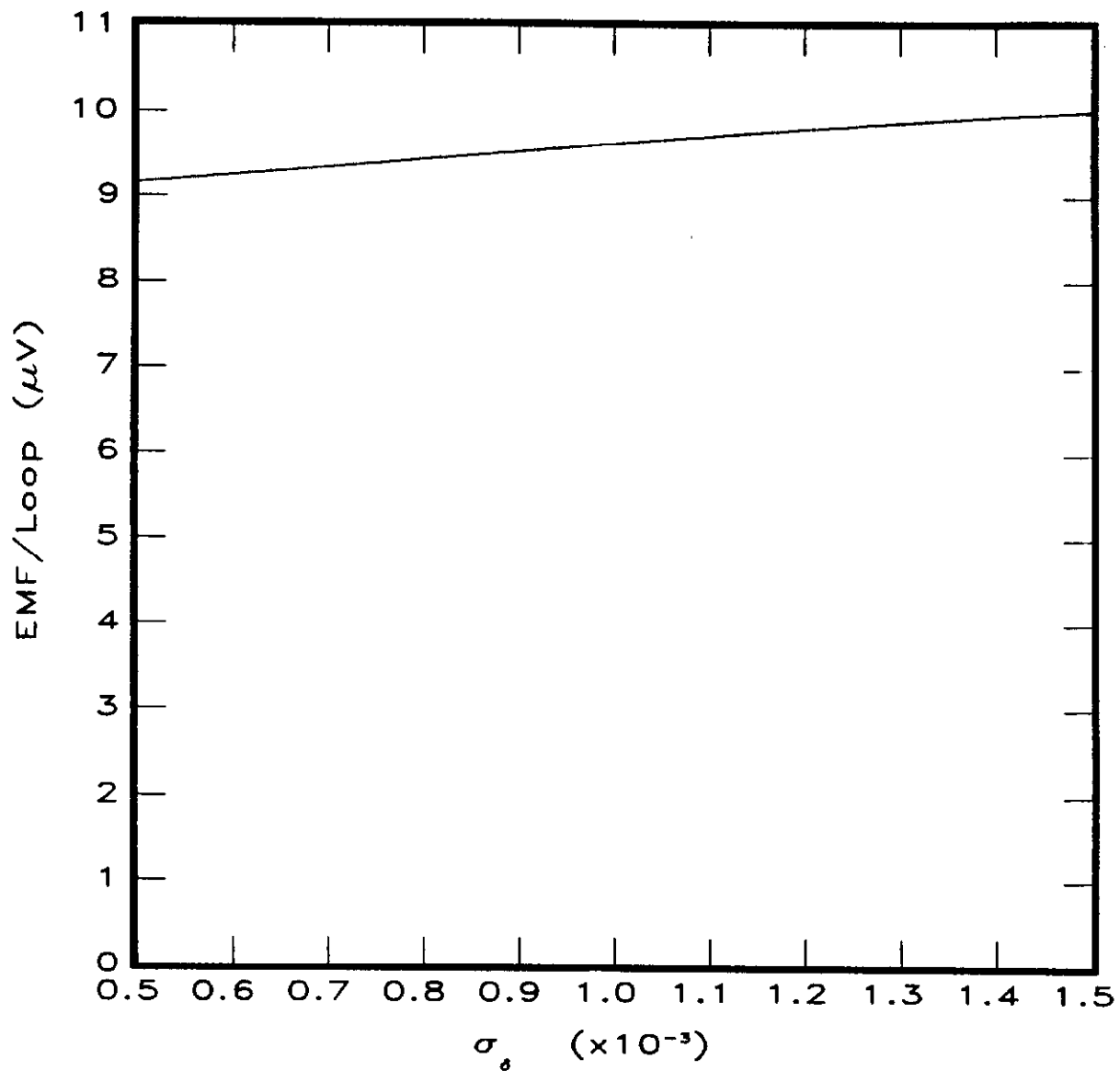


Figure 4.6: Dependence of the maximum voltage induced in a single F13 XIEM detector loop on the bunch fractional energy spread.

Label the loops shown in the beam's eye detector view in figure 4.1 by their quadrant number. Since the transverse emittance signal is odd in both transverse planes, the combination of connections between the four loops which produces a voltage linear in transverse emittance can be written as

$$V_{\text{XIEM}} = V_1 - V_2 + V_3 - V_4 \quad . \quad (4.3)$$

If the beam has a horizontal or vertical angle error through the detector, the loop combinations that would sense this are

$$\begin{aligned} V_{\text{HORZ}} &= V_1 + V_2 - V_3 - V_4 \quad , \\ V_{\text{VERT}} &= V_1 - V_2 - V_3 + V_4 \quad . \end{aligned} \quad (4.4)$$

As long as there were no beam position errors, these three voltage combinations would be sufficient to yield the bunch emittances and angle errors. The magnitude of V_{HORZ} and V_{VERT} can be up to two orders of magnitude greater than V_{XIEM} , when steering errors approach 1 mrad.

Realistically, beam position errors are a fact of life. As the horizontal and vertical beam offsets increase, the contamination of V_{XIEM} with beam steering induced voltages increases quite dramatically. The next section is a discussion of the compensation scheme proposed to negate this effect.

C. Steering Error Compensation

When $x_0, y_0 \gg \sigma_x, \sigma_y$, the portion of the longitudinal magnetic field induced by the beam via steering mismatch can be well approximated by replacing the bunch with a thin wire. Assume a wire with position and angle

errors (x, x', y, y') carries a Gaussian current distribution. The longitudinal component of the magnetic field it generates is given by

$$B_s(x_0, y_0, t) = \frac{\mu_0}{4\pi} \frac{2 Ne}{\sqrt{2\pi} \sigma_\tau} e^{-t^2/2\sigma_\tau^2} \frac{y'(x-x_0) - x'(y-y_0)}{(x-x_0)^2 + (y-y_0)^2} \quad (4.5)$$

Applying equation 4.1 to equation 4.5 yields the induced EMF per loop, per turn, of

$$V(t) = \frac{\mu_0}{4\pi} \frac{2 Ne}{\sqrt{2\pi} \sigma_\tau} \frac{t}{\sigma_\tau} e^{-t^2/2\sigma_\tau^2} \left[(y'x - x'y)I_1 + x'I_s - y'I_c \right] \quad (4.6)$$

where the integrals

$$I_1 = \int_{R_0}^{R_1} dr \int_{\theta_0}^{\theta_1} d\theta \frac{r}{(x - r\cos\theta)^2 + (y - r\sin\theta)^2}$$

$$I_s = \int_{R_0}^{R_1} dr \int_{\theta_0}^{\theta_1} d\theta \frac{r^2 \sin\theta}{(x - r\cos\theta)^2 + (y - r\sin\theta)^2} \quad (4.7)$$

$$I_c = \int_{R_0}^{R_1} dr \int_{\theta_0}^{\theta_1} d\theta \frac{r^2 \cos\theta}{(x - r\cos\theta)^2 + (y - r\sin\theta)^2}$$

depend on the detector loop geometry and the position of the wire (bunch) with respect to the center of the detector. The limits of integration simply signify an integral over a loop, across its full azimuth and radial depth. The evaluation of the integrals is straightforward, but messy. The leading order solution of equations 4.6 and 4.7 is

$$V(t) = \frac{\mu_0}{4\pi} \frac{2 N e t}{\sqrt{2\pi} \sigma_x^2 \sigma_y^2} e^{-t^2/2\sigma_\tau^2} \left[x' L_x(x) - y' L_y(y) \right] \quad (4.8)$$

$$L_x(x) = (R_1 - R_0) (\cos\theta_1 - \cos\theta_0) + x (\sin^2\theta_1 - \sin^2\theta_0) \ln(R_1/R_0)$$

$$L_y(y) = (R_1 - R_0) (\sin\theta_1 - \sin\theta_0) + y (\sin^2\theta_1 - \sin^2\theta_0) \ln(R_1/R_0)$$

Figure 4.7 is a plot of equation 4.8 (summing up all four loops according to equation 4.3) and the result of a calculation of the full blown bunch position and angle dependence. Over the range of reasonable bunch position errors, assuming a reasonably large angle error, the agreement is amazingly good.

The angles x' and y' can be measured directly by the XIEM detector using equation 4.4. By including electrostatic beam detector buttons in the same XIEM package and doing the required signal processing, the beam positions x and y can also be measured. By supplying this information to equation 4.8 and subtracting the result from V_{XIEM} , the XIEM detector can give high accuracy emittance results for beam errors up to fractions of a milliradian and up to a centimeter. Main Ring position fluctuations are well below these limits¹.

1. R. Gerig, Private Communication.

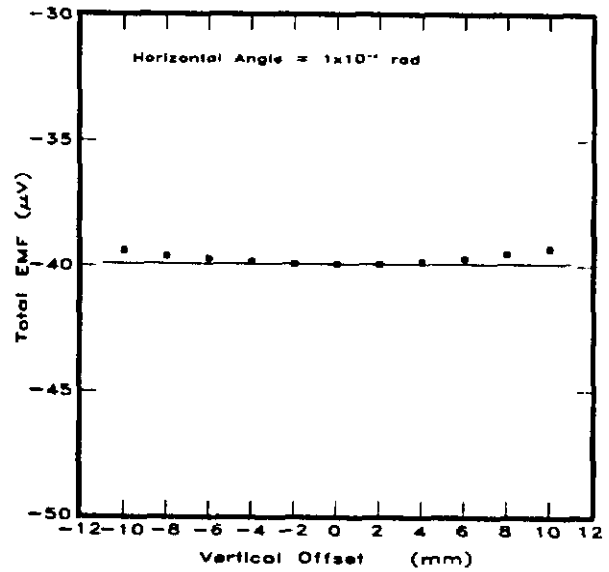
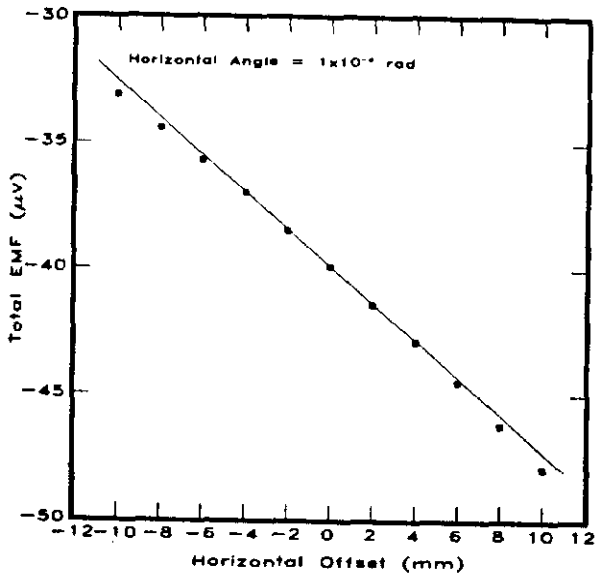
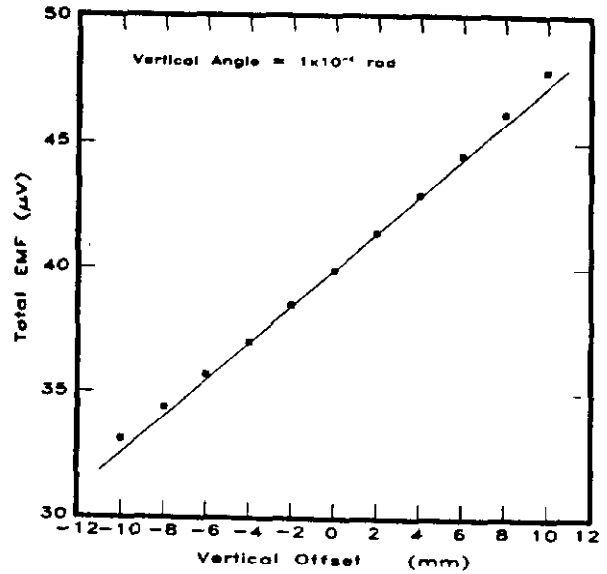
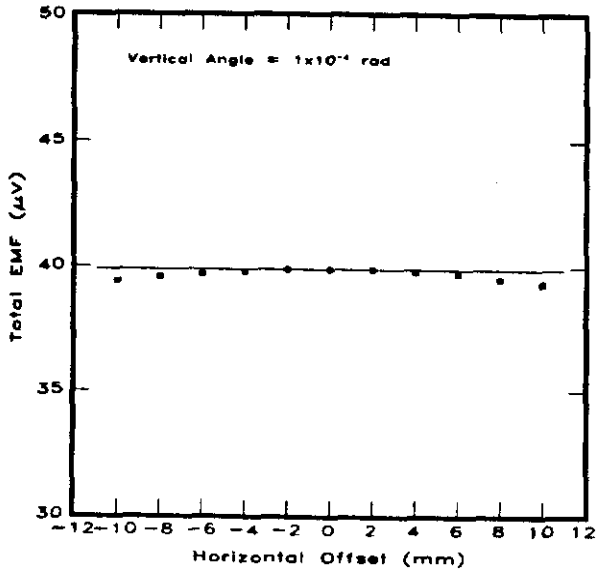


Figure 4.7: The sensitivity of the transverse emittance signal to beam steering and position errors. The points are the calculated sensitivity, while the lines represent the sensitivity estimation from equation 4.8. The agreement is quite good for reasonable beam position errors.

D. Signal Processing

The question most asked concerning this scheme is: Is there enough signal? Given that low noise, wide bandwidth amplifiers exist, the fundamental aspect of this question concerns the signal-to-noise ratio of the conductor loops. The thermal noise voltage at the output taps of a loop is equal to

$$V_n = \sqrt{4 kT R \Delta f} \quad (4.9)$$

Assuming a 10 gauge copper loop, the resistance at room temperature is roughly 0.002 Ω . At a bandwidth of 4 GHz, the noise voltage would be 0.3 μ V. This corresponds to a signal-to-noise ratio of better than 10:1. At a 4 GHz bandwidth, the degradation of the signal from a narrow bunch by a single pole amplifier is shown in figure 4.8. The voltage waveform is reproduced quite well.

A 10 μ V signal is too small to transmit up cables to amplifiers outside the tunnel. In addition, multiple conductor turns per loop reduces the available bandwidth by the square of the number of turns (becoming a serious problem at around 10 turns). Therefore, amplification of 60 db to 80 db next to the detectors is necessary. There exist low cost, low noise gallium arsenide Schottky-gate FET's (such as the AT-12535) which would seem to be perfect for this application.

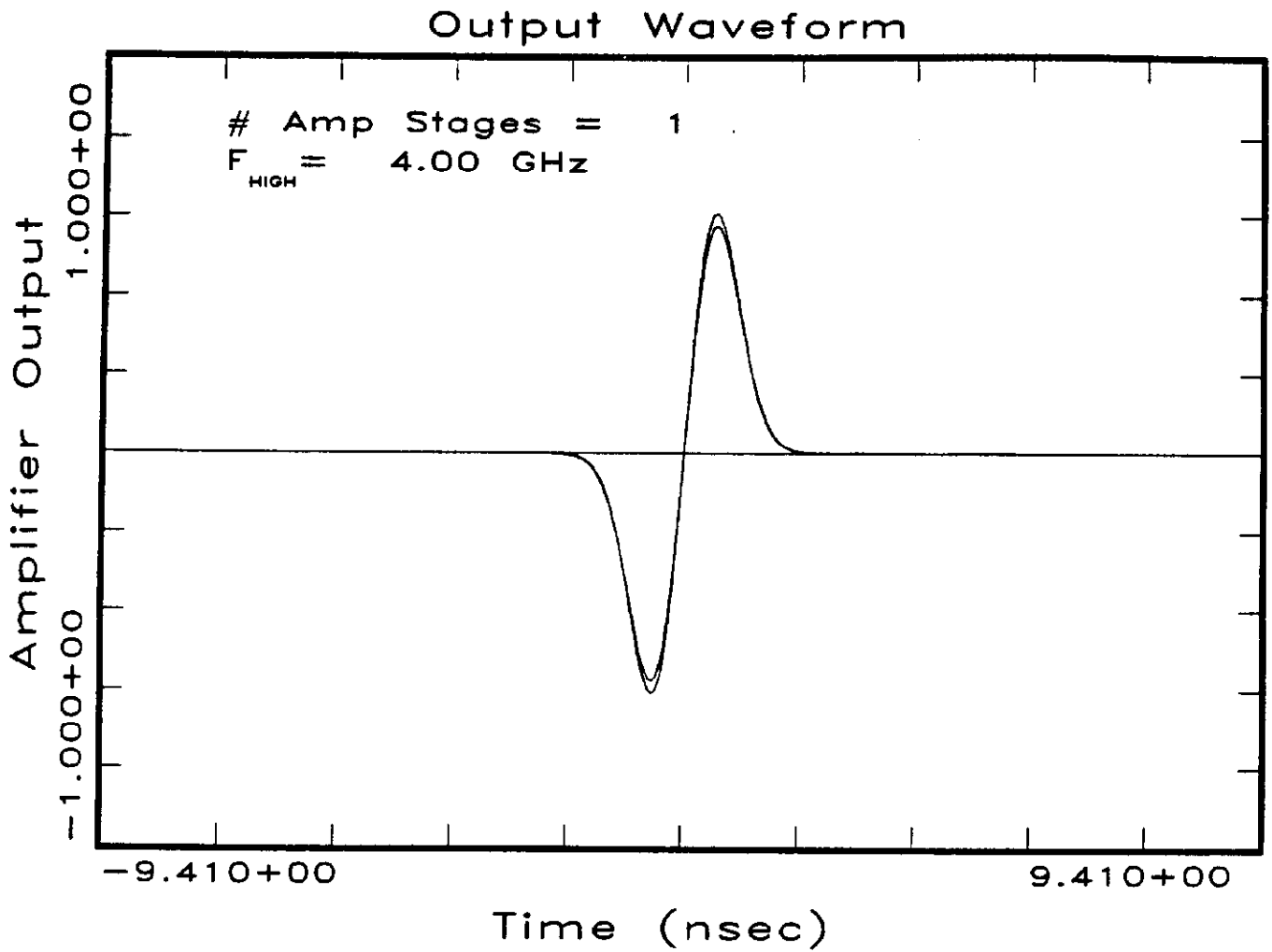


Figure 4.8: The effect of a unity gain amplifier with a 4 GHz single pole bandwidth on a XIEM signal generated by a very short bunch length beam.

V. TEST STAND PROPOSAL

Before placing such an experimental piece of apparatus into an accelerator, a number of questions must be answered. Therefore, it would be a good idea to make bench models of the detector and electronics for test purposes. The subject matter to be addressed by such a project are:

1. Equation verification
2. Effect of beam pipe wall
3. Effect of transition piece
4. Testing beam button performance
5. Test electronics
6. Investigate construction tolerances
6. Investigate long term stability (temperature, vibration, ...)